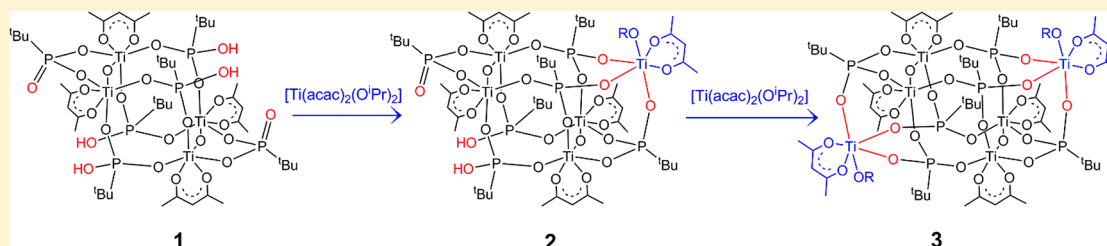


# Complex Structural Landscape of Titanium Organophosphonates: Isolation of Structurally Related $Ti_4$ , $Ti_5$ , and $Ti_6$ Species and Mechanistic Insights

Kamna Sharma, Rajendran Antony, Alok Ch. Kalita, Sandeep Kumar Gupta,<sup>1</sup> Paul Davis, and Ramaswamy Murugavel\*<sup>1</sup>

Department of Chemistry, Indian Institute of Technology Bombay, Powai, Mumbai 400076, India

## Supporting Information



**ABSTRACT:**  $[Ti(acac)_2(OiPr)_2]$  reacts with *tert*-butylphosphonic acid to yield a series of titanium organophosphonates such as tetranuclear  $[Ti_4(acac)_4(\mu-O)_2(\mu-tBuPO_3)_2(\mu-tBuPO_3H)_4] \cdot 2CH_3CN$  (1), pentanuclear  $[Ti_5(acac)_5(\mu-O)_2(OiPr)(\mu-tBuPO_3)_4(\mu-tBuPO_3H)_2]$  (2), hexanuclear  $[Ti_6(acac)_6(\mu-O)_2(OiPr)_2(\mu-tBuPO_3)_6]$  (3), or  $[Ti_6(acac)_6(\mu-O)_3(OiPr)(\mu-tBuPO_3)_5(\mu-tBuPO_3H)] \cdot 2CH_3CN$  (4). The isolation of each of these products in pure form depends on the molar ratio of the reactants or the solvent medium. Among these, 3 is obtained as the only product when the reaction is conducted in  $CH_2Cl_2$ . The structural analysis reveals that a simple cluster growth route relates the clusters 1–4 to each other and that a reactive cyclic single-4-ring titanophosphonate  $[Ti(acac)(OiPr)_2(tBuPO_3H)]_2$  is the fundamental building block. While the tetranuclear 1 has structural resemblance to the D4R building block of zeolites, the hexanuclear clusters 3 and 4 have the shape of zeolitic D6R building blocks. The presence of adventitious water in the phosphonic acid (arising from small quantities of hydrogen-bonded water) results in the formation of  $\mu-O^{2-}$  bridges across an adjacent pair of titanium centers in clusters 1–4. To further verify the stability of the hexanuclear cluster over other structural forms, the reaction of  $tBuPO_3H_2$  was performed with  $[Ti(acac)_2(O)]$ , instead of  $Ti(acac)_2(OiPr)_2$ , in  $CH_3CN$  to yield  $[Ti_6(acac)_6(\mu-O)_4(\mu-tBuPO_3)_4(\mu-tBuPO_3H)_2] \cdot 2CH_3CN$  (5). Compound 5 exhibits a core structure similar to those of 3 and 4 with small variations in the intracuster Ti–O–Ti linkage. Compound 3 is an efficient and selective catalyst for olefin epoxidation under both homogeneous and heterogeneous conditions.

## INTRODUCTION

Among the catalytically active metals, titanium is of special interest due to high abundance and low toxicity. Titanium-doped zeolites and silicates are efficient catalysts in many organic transformations, notably olefin oxidation and hydroxylation of phenols.<sup>1</sup> Several organic-soluble molecular titanosilicates have been synthesized using different titanium precursors and organosilanols ( $RSi(OH)_3$  or  $R_2Si(OH)_2$ ), exhibiting different nuclearities with different coordination geometries around the titanium metal ion.<sup>1b,i,2</sup> Selections of these discrete titanosiloxanes have been transformed into high-titanium-content titanosilicate materials and used in several organic oxidation reactions.<sup>2b</sup> Similar to the case for organosilanols, phosphonic acids ( $RPO_3H_2$ ) and phosphinic acids ( $R_2PO_2H$ ) have also been used to prepare structurally diverse discrete titanium clusters due to both structural and functional similarities between silicate and phosphonate clusters in many instances.<sup>3</sup> Different phosphonic acids have been reported to form structurally diverse titanium clusters with different nuclearities under different reaction conditions.<sup>4</sup> The first

examples of organic-soluble molecular titanium phosphonate cages  $[(Cp^*TiO_3PR)_4(\mu-O)_2]$  ( $R = Me, Ph$ ) and  $[(Cp^*Ti)_3(tBuPO_3)_2\{tBuPO_2(OH)\}(\mu-O)_2]$  were reported by Roesky and co-workers from the reaction of  $Cp^*TiMe_3$  with phosphonic acids.<sup>5</sup> These molecules can be considered as secondary building units (SBUs) for the eventual preparation of solid-state titanophosphate materials.<sup>6</sup> They also reported on the synthesis of eight-membered dititanophosphonate rings  $[(OiPr)_3Ti(\mu-O)_2PPh_2]_2$  and  $[(OiPr)_3Ti(\mu-O)_2P(tBu)(OSiMe_3)]_2$ .<sup>7</sup> Around the same time Mehring et al. reported on the reactions of titanium isopropoxide with  $RP(O)(OH)_2$  ( $R = Ph, Me, tBu, 4-NCC_6H_4$ ) in DMSO, resulting in the isolation of  $[Ti_4(\mu_3-O)(OiPr)_5(\mu-OiPr)_3(RPO_3)_3] \cdot DMSO$ .<sup>8</sup> These compounds are the first examples of Ti oxo-alkoxides modified by tridentate phosphonates ( $RPO_3^{2-}$ ). The reaction of titanium isopropoxide with *tert*-butylphosphonic acid under

Received: June 28, 2017

rigorous exclusion of water (in toluene) gave the titanium phosphonate tetramer  $[\text{Ti}(\text{O}^i\text{Pr})_2(\text{tBuPO}_3)_4]$ .<sup>8a</sup>

Further, different phosphonic acids can change or modulate the nuclearity of the resulting cluster, depending on the nature of the phosphonic acid substituent. For example, the reaction of allylphosphonic acid with titanium isopropoxide in DMSO results in a tetrameric cluster, but bis(trimethylsilyl)-allylphosphonate reacts with titanium isopropoxide in isopropyl alcohol to yield an octanuclear cluster.<sup>9</sup> Similarly, bis(trimethylsilyl)phosphonates  $\text{RP}(\text{O})(\text{OSiMe}_3)_2$  (R = ethyl, 3-chloropropyl, benzyl, 3,5-dimethylphenyl, 2-naphthylmethyl) react with titanium isopropoxide to give octa-, hepta-, or tetranuclear clusters.<sup>9</sup> Use of similar phosphonates in reactions with titanium isopropoxide in the presence of acetic acid resulted in hexanuclear oxo clusters.<sup>10</sup> In case of R = 2-bromopropyl, xylyl, the same reaction yields the pentanuclear cluster  $[\text{Ti}_5\text{O}(\text{O}^i\text{Pr})_{11}(\text{OAc})(\text{O}_3\text{PR})_3]$ .<sup>11</sup> The use of hydrothermal methods for the reaction of phenylphosphonic acid with titanium ethoxide in ethanol resulted in a tetrameric cluster which has been used to synthesize polyoxotitanate nanoclusters  $\text{Ti}_{25}$  and  $\text{Ti}_{26}$  in the presence of an ammonium salt.<sup>12</sup> Similarly, *tert*-butylphosphonic acid forms dimeric, trimeric, and tetrameric titanium clusters on reacting with titanium methoxide,  $\text{Cp}^*\text{TiMe}_3$ , and titanium isopropoxide, respectively.<sup>5,8a,13</sup>

Organophosphate ligands can replace phosphonates to yield even more structurally diverse titanium clusters.<sup>14–16</sup> For example, the reaction of  $\text{Ti}(\text{OSiMe}_3)_4$  with di-*tert*-butylphosphate in hexane resulted in the tetrameric titanium complex  $[\text{TiO}(\text{SiMe}_3)(\text{O}_2\text{P}(\text{O}^t\text{Bu}))_2]_4$  similar to D4R SBUs observed in zeolites.<sup>14</sup> The same phosphate ligand reacts with titanium alkoxide to give dimeric complexes  $[\text{Ti}(\text{OR})_3(\text{O}_2\text{P}(\text{O}^t\text{Bu}))_2]_2$  (R = Et, <sup>*i*</sup>Pr).<sup>14</sup> The addition of KOEt to a solution of  $[\text{Ti}(\text{OEt})_3(\text{O}_2\text{P}(\text{O}^t\text{Bu}))_2]_2$  leads to the formation of a potassium-containing titanium phosphate,  $[\text{Ti}_2\text{K}(\text{OEt})_8(\text{O}_2\text{P}(\text{O}^t\text{Bu}))_2]_2$ ,<sup>8a</sup> which is a centrosymmetric dimer in the solid state.<sup>15</sup>

Hence, it is evident from the structural diversity that the structure of the clusters has a profound influence on the choice of the titanium precursor as well as the steric requirements or the nature of the organic substituent on phosphorus.<sup>17</sup> Even when the substituent on the phosphorus is kept the same (e.g., <sup>*t*</sup>BuPO<sub>3</sub>H<sub>2</sub>), just by changing the source of titanium (e.g.,  $\text{Ti}(\text{O}^i\text{Pr})_4$  or  $\text{Cp}^*\text{TiMe}_3$ ) and controlling the presence or absence of adventitious water in the reaction system, one can isolate different structural types.<sup>5,8a</sup>

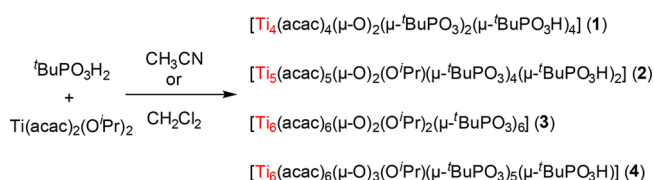
The present study hence is aimed at probing the structural landscape of titanium phosphonates in detail and establishing a reaction pathway and, if possible, even a mechanism for the formation and growth of these clusters in a given reaction medium under identical reaction conditions. Although there is a clear advantage in either using an organometallic precursor such as  $\text{Cp}^*\text{TiMe}_3$  (eliminating alkane as byproduct) or using an alkoxide such as titanium isopropoxide (the byproduct is an alcohol), we have used in the present study  $[\text{Ti}(\text{acac})_2(\text{O}^i\text{Pr})_2]$ , which contains both chelating diketonate and terminal alkoxide ligands. Such attempts to modify the titanium centers using similar bidentate ligands without seriously impairing the reactivity at the metal center has precedence in the literature.<sup>9–11,18</sup> A further likely advantage of using  $[\text{Ti}(\text{acac})_2(\text{O}^i\text{Pr})_2]$  may stem from the possible stabilization of six-coordinate titanium centers in the resultant clusters, which is in stark contrast to the earlier reported titanium *tert*-

butylphosphonates, most of which contain titanium in a pentacoordinate state.

## RESULTS AND DISCUSSION

**Reactivity of  $[\text{Ti}(\text{acac})_2(\text{O}^i\text{Pr})_2]$  with <sup>*t*</sup>BuPO<sub>3</sub>H<sub>2</sub>.** A detailed investigation of the reactivity of  $[\text{Ti}(\text{acac})_2(\text{O}^i\text{Pr})_2]$  with *tert*-butylphosphonic acid has been carried out in two different solvents (acetonitrile and dichloromethane), resulting in the isolation of a series of titanium phosphonate clusters. While the reactions carried out in acetonitrile seemed to be highly dependent on the ratio of the reactants and amount of the solvent used, yielding tetranuclear, pentanuclear, and hexanuclear titanophosphonate clusters **1**, **2**, and **4**, the runs carried out in dichloromethane invariably produced the hexanuclear cluster **3** (Scheme 1). The isolation of multiple

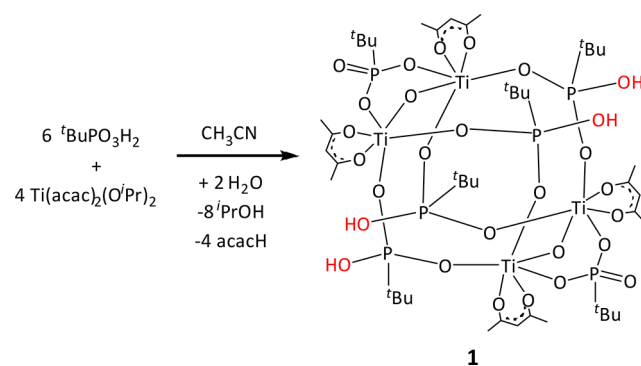
**Scheme 1. Complex Reaction of  $[\text{Ti}(\text{acac})_2(\text{O}^i\text{Pr})_2]$  with <sup>*t*</sup>BuPO<sub>3</sub>H<sub>2</sub> in CH<sub>3</sub>CN or CH<sub>2</sub>Cl<sub>2</sub>**



products in the reactions carried out in acetonitrile is also the result of variable amounts of adventitious water present in the reaction medium. Hence, these reactions were carefully optimized to isolate any one of the three products in a given run. Further, since all the four isolated clusters seem to have formed through a common building block (a single-4-ring), a detailed mechanism for the growth of titanium phosphonates clusters is also presented.

$[\text{Ti}_4(\text{acac})_4(\mu\text{-O})_2(\mu\text{-tBuPO}_3)_2(\mu\text{-tBuPO}_3\text{H})_4] \cdot 2\text{CH}_3\text{CN}$  (**1**). The reaction of  $[\text{Ti}(\text{acac})_2(\text{O}^i\text{Pr})_2]$  with *tert*-butylphosphonic acid in a 1:1.5 ratio using acetonitrile as solvent gives the tetranuclear titanium phosphonate **1**, as shown in Scheme 2.

**Scheme 2. Synthesis of  $[\text{Ti}_4(\text{acac})_4(\mu\text{-O})_2(\mu\text{-tBuPO}_3)_2(\mu\text{-tBuPO}_3\text{H})_4] \cdot 2\text{CH}_3\text{CN}$  (**1**)**



The titanium precursor has been added to the suspension of phosphonic acid in acetonitrile at room temperature under an inert atmosphere and filtered to obtain a clear solution after stirring for 12 h. Pale yellow single crystals of **1** suitable for X-ray diffraction have been obtained over a period of 20 days from this solution and characterized by spectroscopic and analytical techniques, in addition to a single-crystal X-ray diffraction study.

The FT-IR spectrum exhibits carbonyl stretching vibrations of the acetylacetonate at  $1605\text{ cm}^{-1}$ . The strong characteristic Ti–O–P stretching has been observed at  $1139$  and  $1075\text{ cm}^{-1}$  (Figure S1 in the Supporting Information). The TGA trace of **1** (Figure S6 in the Supporting Information) shows that compound **1** is stable up to  $100\text{ }^{\circ}\text{C}$ . Compound **1** crystallizes in the monoclinic  $P2_1/c$  space group. A perspective view of the full molecule and the molecular core of **1** is shown in Figure 1.

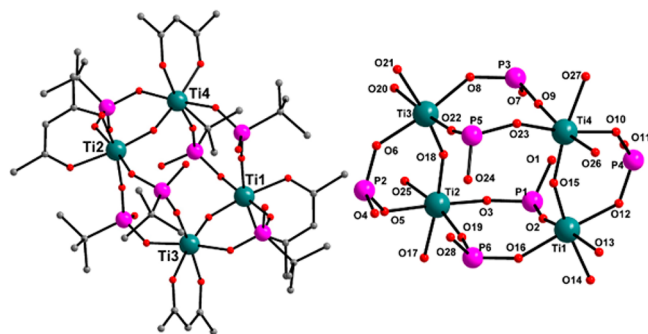


**Figure 1.** (left) Molecular structure of  $[\text{Ti}_4(\text{acac})_4(\mu\text{-O})_2(\mu\text{-}^t\text{BuPO}_3)_2(\mu\text{-}^t\text{BuPO}_3\text{H})_4]\cdot 2\text{CH}_3\text{CN}$  (**1**). Hydrogen atoms are omitted for clarity. (right) Core structure of **1**.

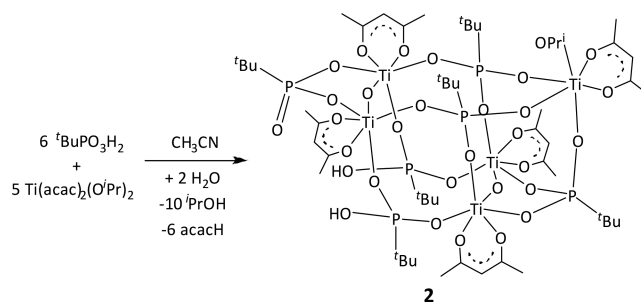
Titanophosphonate **1** is a tetranuclear cluster incorporating two fully deprotonated phosphonate, four monodeprotonated phosphonate, four acetylacetonate (acac), and two  $\mu_2\text{-O}$  functionalities. Two solvent acetonitrile molecules are present in the lattice. Molecule **1** exists as a discrete entity with no interaction with the neighboring molecules. Each titanium metal ion in **1** exists in a distorted-octahedral geometry (bond angles at the metal range between  $81.8$  and  $176.8^\circ$ ). All six phosphonate ligands in the cluster behave as bidentate ligands (Harris notation: [2.110]). The titanium metal ion is bonded to six oxygen atoms, two of which are from acac (equatorial plane) and three are from phosphonic acid (one at the equatorial plane and two at axial positions). The sixth coordination site is taken up by a  $\mu_2\text{-oxide}$  anion that forms a bridge with the neighboring titanium center (equatorial plane).

$[\text{Ti}_5(\text{acac})_5(\mu\text{-O})_2(\text{O}^i\text{Pr})(\mu\text{-}^t\text{BuPO}_3)_4(\mu\text{-}^t\text{BuPO}_3\text{H})_2]$  (**2**). Complex **2** was formed when only a slight excess of  $[\text{Ti}(\text{acac})_2(\text{O}^i\text{Pr})_2]$  was used for the reaction with  $^t\text{BuPO}_3\text{H}_2$  (5:6 molar ratio) in acetonitrile with constant stirring at room temperature. From the resulting reaction mixture, pale yellow crystals of **2** were isolated over a period of 7 days. Although this reaction has been repeated several times under almost identical conditions, cluster **2** was obtained as the product only in a couple of instances, while cluster **4** has been obtained in other instances in view of the close structural relationship between them (vide infra).

Due to the insolubility of cluster **2**, it has been characterized only in the solid state by elemental analysis and IR spectroscopy (see the Experimental Section), apart from its molecular structure determination by single-crystal X-ray diffraction studies. The quality of the crystals obtained for compound **2** was rather poor (flakelike), and hence the structure refinement converged at a slightly higher  $R$  factor of 10.58%.

The molecular structure of **2** can be viewed as an addition product of **1** with 1 equiv more of  $\text{Ti}(\text{acac})_2(\text{O}^i\text{Pr})_2$  (Scheme 3). A positional disorder with 0.5 site occupancy for the fifth  $\text{Ti}(\text{acac})_2(\text{O}^i\text{Pr})$  unit is observed in its molecular structure. This

### Scheme 3. Synthesis of $[\text{Ti}_5(\text{acac})_5(\mu\text{-O})_2(\text{O}^i\text{Pr})(\mu\text{-}^t\text{BuPO}_3)_4(\mu\text{-}^t\text{BuPO}_3\text{H})_2]$ (**2**)



disorder can be better understood by invoking a simple model depicted in Figure 2. Thus, the structure of **2** can be described

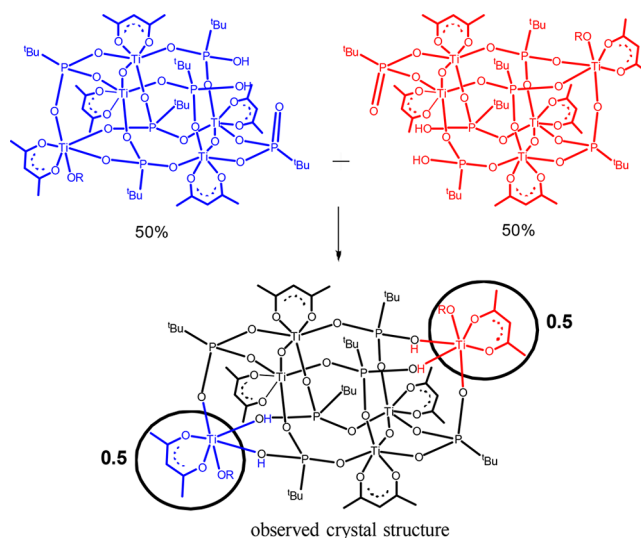


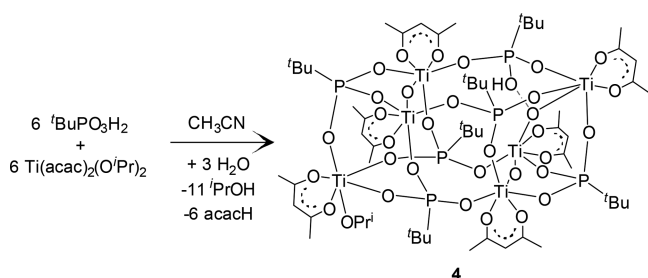
**Figure 2.** Schematic representation of the positional disorder of the  $\text{Ti}(\text{acac})(\text{O}^i\text{Pr})$  unit in the crystal of **2**. In the bottom molecule, the atoms within the encircled portion (shown in red and blue) exhibit a SOF of 0.5, while the rest of the molecule shown in black has a SOF of 1.0.

as a pentanuclear titanophosphonate cluster incorporating six phosphonate (four fully deprotonated and two monodeprotonated), five acetylacetonate, one alkoxide, and two  $\mu_2\text{-O}$  functionalities. All five titanium centers in the molecule exist in a distorted-octahedral geometry. Two pairs of titanium ions are bridged by  $\mu_2\text{-O}$ , while the phosphonate group binds in a tridentate fashion. Other bond lengths and angles around titanium are similar to those found for **1**.

$[\text{Ti}_6(\text{acac})_6(\mu\text{-O})_3(\text{O}^i\text{Pr})(\mu\text{-}^t\text{BuPO}_3)_5(\mu\text{-}^t\text{BuPO}_3\text{H})]\cdot 2\text{CH}_3\text{CN}$  (**4**). The reaction of  $[\text{Ti}(\text{acac})_2(\text{O}^i\text{Pr})_2]$  with *tert*-butylphosphonic acid in acetonitrile in a 1:1 stoichiometry gives the hexanuclear complex  $[\text{Ti}_6(\text{acac})_6(\mu\text{-O})_3(\text{O}^i\text{Pr})(\mu\text{-}^t\text{BuPO}_3)_5(\mu\text{-}^t\text{BuPO}_3\text{H})]\cdot 2\text{CH}_3\text{CN}$  (**4**) as pale yellow crystals (Scheme 4). Compound **4** has been fully characterized by analytical and spectroscopic techniques and a single-crystal X-ray diffraction study. Compound **4** is the most stable form of the three different clusters (**1**, **2**, or **4**) obtained from the reactions conducted in acetonitrile.

A single-crystal X-ray diffraction study reveals that compound **4** crystallizes in the monoclinic  $P2_1/c$  space group. A perspective view of the molecular structure and core of  $[\text{Ti}_6(\text{acac})_6(\mu\text{-O})_3(\text{O}^i\text{Pr})(\mu\text{-}^t\text{BuPO}_3)_5(\mu\text{-}^t\text{BuPO}_3\text{H})]\cdot 2\text{CH}_3\text{CN}$

**Scheme 4. Synthesis of  $[\text{Ti}_6(\text{acac})_6(\mu\text{-O})_3(\text{O}^i\text{Pr})(\mu\text{-}^t\text{BuPO}_3)_5(\mu\text{-}^t\text{BuPO}_3\text{H})]\cdot 2\text{CH}_3\text{CN}$  (4)**



(4) is shown in Figure 3. In a sense, compound 4 can be considered as a further grown version of 2 through the

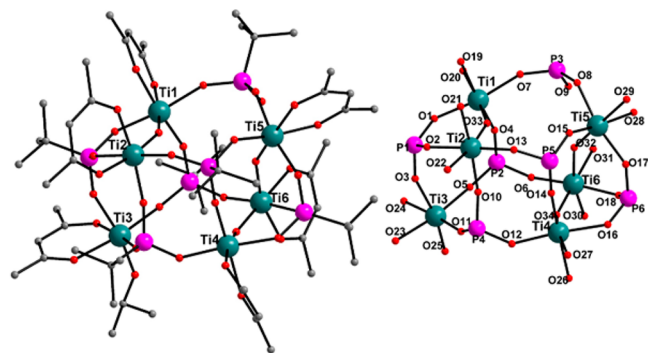


**Figure 3.** (left) Molecular structure of  $[\text{Ti}_6(\text{acac})_6(\mu\text{-O})_3(\text{O}^i\text{Pr})(\mu\text{-}^t\text{BuPO}_3)_5(\mu\text{-}^t\text{BuPO}_3\text{H})]\cdot 2\text{CH}_3\text{CN}$  (4). Hydrogen atoms are omitted for clarity. (right) Core structure of 4.

attachment of a second  $[\text{Ti}(\text{acac})(\text{O}^i\text{Pr})]$  unit to the cluster 2. In other words, 4 is formed by double titanium capping of the original tetrameric cluster 1. Thus, the hexanuclear 4 consists of six phosphonate, six acetylacetonate (acac), one  $\text{O}^i\text{Pr}$ , and three  $\mu_2\text{-O}$  functionalities. All six titanium centers exist in a distorted-octahedral geometry, albeit with different coordination environments.

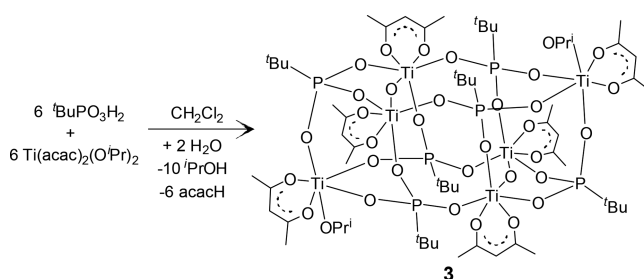
Ti1 is coordinated by two oxygen atoms of acac, one oxygen of a partially deprotonated phosphonate ligand, two oxygens of fully deprotonated phosphonate, and one  $\mu_2\text{-O}$  which bridges Ti1 to Ti2. The other five coordination sites of Ti2 are occupied by one acac chelate and three fully deprotonated phosphonate ligands. Ti3 is bound to one acac, three deprotonated phosphonates, and one isopropoxide. Ti4 is found to be coordinated to one acac ligand, three deprotonated phosphonates, and one  $\mu_2\text{-O}$  which bridges Ti4 to Ti6. The six-coordinate Ti5 metal center is coordinated to one acac and one partially deprotonated and two fully deprotonated phosphonate ligands apart from one  $\mu_2\text{-O}$  which bridges it to Ti6. Thus, Ti6 is the only titanium center in the molecule that is surrounded by two  $\mu_2\text{-O}$  bridges (Ti4 and Ti5) apart from being surrounded by one acac ligand and two deprotonated phosphonate ligands.

Although the structure of 4 may appear very symmetric at first sight, the possible loss of isopropoxide from Ti5 (diagonally opposite to Ti3), though hydrolysis and subsequent formation of an additional  $\text{Ti-O-Ti}$  bridge, render this cluster less symmetric. Hence, as the hydrolysis of an isopropoxide seems to be the essential cause of the symmetry lowering, the above reaction was repeated in the less hygroscopic dichloro-

methane to yield the missing symmetric hexamer 3, which is described below.

$[\text{Ti}_6(\text{acac})_6(\mu\text{-O})_2(\text{O}^i\text{Pr})_2(\mu\text{-}^t\text{BuPO}_3)_6]$  (3). Since the reaction of  $^t\text{BuPO}_3\text{H}_2$  with  $[\text{Ti}(\text{acac})_2(\text{O}^i\text{Pr})_2]$  yielded as many as three different clusters, 1, 2, and 4 (see below), in acetonitrile with different nuclearities, the same reaction was repeated in dichloromethane with the aim of controlling the adventitious water in the reaction mixture (vide supra). Thus, the reaction of  $[\text{Ti}(\text{acac})_2(\text{O}^i\text{Pr})_2]$  with *tert*-butylphosphonic acid in dichloromethane gives the hexanuclear titanium complex  $[\text{Ti}_6(\text{acac})_6(\mu\text{-O})_2(\text{O}^i\text{Pr})_2(\mu\text{-}^t\text{BuPO}_3)_6]$  (3) as pale yellow crystals, as shown in Scheme 5. Compound 3 has been fully characterized by using analytical and spectroscopic techniques, and structure determination was done by a single-crystal X-ray diffraction study.

**Scheme 5. Synthesis of  $[\text{Ti}_6(\text{acac})_6(\mu\text{-O})_2(\text{O}^i\text{Pr})_2(\mu\text{-}^t\text{BuPO}_3)_6]$  (3)**



X-ray diffraction studies reveal that the compound  $[\text{Ti}_6(\text{acac})_6(\mu\text{-O})_2(\text{O}^i\text{Pr})_2(\mu\text{-}^t\text{BuPO}_3)_6]$  (3) is a novel  $\text{Ti-O-P}$  cluster, which crystallizes in the monoclinic  $P2_1/n$  space group. A perspective view of the molecular structure and the core structure of 3 are shown in Figure 4.

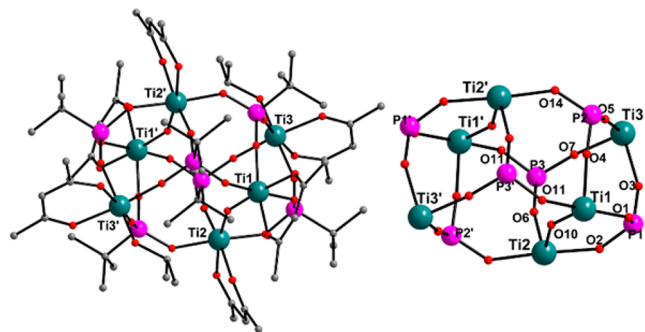


**Figure 4.** (left) Molecular structure of  $[\text{Ti}_6(\text{acac})_6(\mu\text{-O})_2(\text{O}^i\text{Pr})_2(\mu\text{-}^t\text{BuPO}_3)_6]$  (3). Hydrogen atoms are omitted for clarity. (right) Core structure of 3.

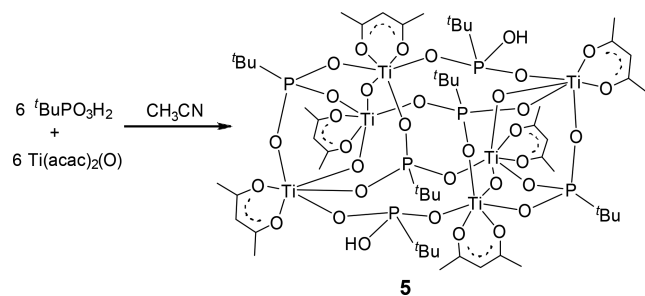
Compound 3 is a drum-shaped symmetric hexatitanophosphonate cluster incorporating six phosphonate, six acetylacetonate, two  $\mu_2\text{-O}$ , and two isopropoxide functionalities. The central core, which is  $\text{Ti}_6\text{O}_{20}\text{P}_6$ , consists of six titanium and six phosphorus atoms that occupy the alternate vertices of a drum. The  $\text{Ti}\cdots\text{P}$  edges of this hexagonal drum are bridged by a  $\mu_2\text{-O}$  atom. In the centrosymmetric hexanuclear cluster, all titanium centers exist in a distorted-octahedral geometry. Ti1 and Ti2 centers display an almost identical coordination geometry where the metal ions are surrounded by three phosphonate oxygen atoms, one acac ligand, and a bridging oxide that connects these two metal ions. The third metal center lacks the

bridging oxide ion but is bound by a terminal monodentate isopropoxide ligand. The six phosphonate ligands bind three metal ions in a [3.111], tridentate fashion.

The FT-IR spectra of **3** and **4** showed carbonyl stretching vibrations of the acetylacetonate at 1596 and 1605  $\text{cm}^{-1}$ , respectively. The strong characteristic Ti–O–P stretching vibrations were observed at 1144 and 1139  $\text{cm}^{-1}$  for **3** and **4**, respectively (Figure S3 in the Supporting Information). The TGA profiles for compounds **3** and **4** are almost similar, as shown in Figure S7 in the Supporting Information. Both compounds are quite stable up to 150 °C. Heating up to 250 °C results in a gradual weight loss corresponding to the removal of coordinated solvent molecules from the crystal lattice. Further heating up to 550 °C results in a weight loss that corresponds to the loss of coligand and the moiety of the phosphonate ligand, leading to the possible formation of inorganic titanium phosphate, which is stable at least up to 1000 °C.

$[\text{Ti}_6(\text{acac})_6(\mu\text{-O})_4(\mu\text{-}^t\text{BuPO}_3)_4(\mu\text{-}^t\text{BuPO}_3\text{H})_2]\cdot 2\text{CH}_3\text{CN}$  (**5**). In order to remove the hydrolysis-prone isopropoxide from the equation and also probe the relative stability of clusters of various nuclearity, the titanium(IV) precursor  $[\text{Ti}(\text{acac})_2(\text{O})]$  has been used as the titanium source in its reaction with the same phosphonic acid  $^t\text{BuPO}_3\text{H}_2$ . An equimolar reaction between these reactants in acetonitrile as solvent results in the isolation of the new cluster complex  $[\text{Ti}_6(\text{acac})_6(\mu\text{-O})_4(\mu\text{-}^t\text{BuPO}_3)_4(\mu\text{-}^t\text{BuPO}_3\text{H})_2]\cdot 2\text{CH}_3\text{CN}$  (**5**), which is also a hexameric titanium cluster (Scheme 6). The product has been obtained in pure form.

#### Scheme 6. Synthesis of $[\text{Ti}_6(\text{acac})_6(\mu\text{-O})_4(\mu\text{-}^t\text{BuPO}_3)_4(\mu\text{-}^t\text{BuPO}_3\text{H})_2]\cdot 2\text{CH}_3\text{CN}$ (**5**)



The FT-IR spectrum of **5** showed a carbonyl stretching vibration of the acetylacetonate at 1597  $\text{cm}^{-1}$ . The strong characteristic absorption bands for Ti–O–P stretching, bending and P=O were observed at 1141, 1024, and 992  $\text{cm}^{-1}$ , respectively (Figure S5 in the Supporting Information). The TGA profile of **5** (Figure S8 in the Supporting Information) shows that the compound is stable up to 150 °C, after which a gradual weight loss occurs due to the loss of coordinated solvent molecule from the crystal lattice. Further heating of the sample up to 550 °C results in the loss of coligand and the organic residuals of the phosphonate ligand leading to the possible formation of inorganic titanium phosphate.

Complex **5** crystallizes in the triclinic  $P\bar{1}$  space group. It is a hexatitanium cluster that is primarily held together by coordination with acetylacetonate and the phosphonate  $^t\text{BuPO}_3$  dianion. Further, **5** exhibits a close structural resemblance to cluster **4** described above. In the asymmetric part of the centrosymmetric unit cell (Figure 5) (which

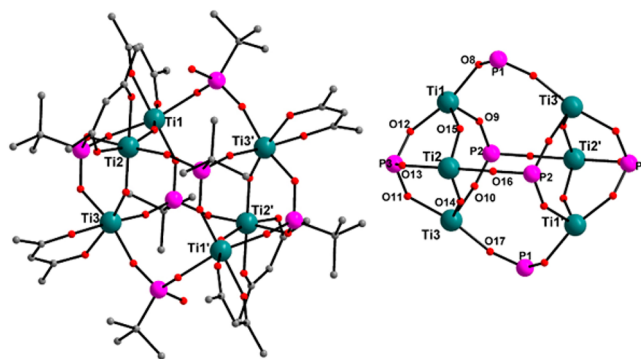


Figure 5. (left) Molecular structure of **5**. Hydrogen atoms are omitted for clarity. (right) Core structure of **5**.

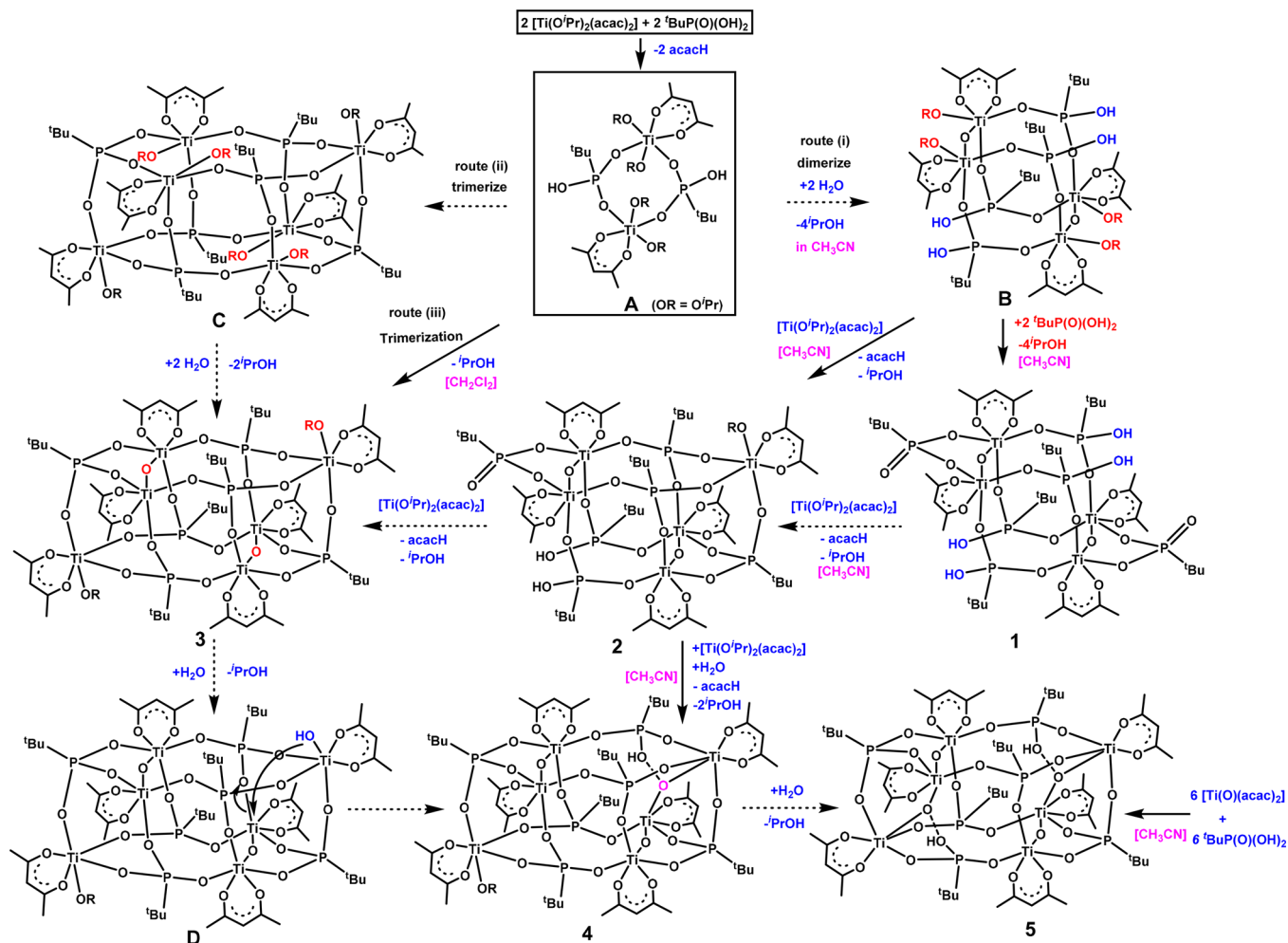
contains only half of the molecule), three titanium metals are present along with three acetylacetonate ligands, two triply bridging  $^t\text{BuPO}_3^{2-}$  dianions, one doubly bridging  $^t\text{BuPO}_3\text{H}^-$ , and two  $\mu_2\text{-O}$  centers that bridge Ti2 to Ti1 and Ti3 (Figure 5, right). Each titanium exists in an octahedral geometry (bond angle range is 80.97–176.48°).

**Plausible Pathway and Mechanistic Insights into the Cluster Formation.** The formation of clusters **1**–**4** and the eventual final product **5** has been rationalized by invoking the plausible pathway shown in Scheme 7. As has been extensively demonstrated in the case of zinc phosphate chemistry,<sup>19</sup> the initial step in the reaction sequence appears to be the formation of the cyclic dimer  $[\text{Ti}_2(\text{acac})_2(\text{O}^i\text{Pr})_4(\mu\text{-}^t\text{BuPO}_3\text{H})_2]$  (**A**) with an S4R core (boxed item in Scheme 7). This initial reaction product can dimerize (route i) or trimerize (route ii) to form  $[\text{Ti}_4(\text{acac})_4(\mu\text{-O})_2(\text{O}^i\text{Pr})_4(\mu\text{-}^t\text{BuPO}_3\text{H})_4]$  (**B**) or  $[\text{Ti}_6(\text{acac})_6(\text{O}^i\text{Pr})_6(\mu\text{-}^t\text{BuPO}_3)_6]$  (**C**), respectively.

The reason for **B** not being isolated as a product can be attributed to the presence of large number of free Ti–O<sup>i</sup>Pr groups. Since the isopropoxide groups are ideally positioned to capture further phosphonic acids, facile formation of product **1** results through the condensation of Ti–O<sup>i</sup>Pr groups with 2 equiv of phosphonic acid. Thus, cluster **1** is rendered phosphorus rich in the process and hence becomes reactive toward further amounts of titanium. If the stoichiometry of titanium can be controlled (which is very difficult), the growth of the cluster can be stopped with only one titanium center added to either of the two reactive faces of **1** to yield the pentanuclear titanium phosphonate **2**. Alternatively, **B** can also simultaneously react with 2 equiv of both phosphonic acid and  $\text{Ti}(\text{acac})_2(\text{O}^i\text{Pr})_2$  in one step to directly yield the pentamer **2**. Ultimately, both routes involve the removal of four molecules of isopropanol and one acacH.

Cluster **2** can be converted to cluster **3** through the reaction of another 1 equiv of titanium precursor. However, repeated reactions carried out in acetonitrile clearly showed that the formation of **4** is preferred to that of **3**. As can be seen from Scheme 7, clusters **3** and **4** are related to each other through a simple hydrolysis of one of the two Ti–O<sup>i</sup>Pr linkages. It is evident that the adventitious water present in the reaction medium drives the reaction all the way to **4**.<sup>20</sup> Switching over to a less hygroscopic (but still polar) solvent such as  $\text{CH}_2\text{Cl}_2$  overcomes this difficulty and yields directly cluster **3** as the only product, probably through the intermediacy of **C**.<sup>20</sup> The only missing link in this sequence of events is the hydrolysis of the second Ti–O<sup>i</sup>Pr group on **3** (or the solitary Ti–O<sup>i</sup>Pr linkage on **4**), to yield **5**. In principle, a 1:1 reaction in a wet solvent

Scheme 7. Plausible Mechanism for the Sequential Formation of 1–5



should proceed all the way by a successive addition–hydrolysis mechanism to yield **5**. As it turns out, this does not happen and the reaction stops at **4**. Thus, the isolation of **5** was finally achieved by starting from a precursor that does not contain any isopropoxide linked to the metal, e.g.  $[\text{Ti}(\text{O})(\text{acac})_2]$ , thus completing the titanium phosphonate jigsaw puzzle described in Scheme 7. In summary, it appears that the titanium phosphonate chemistry is very similar to the zinc phosphate chemistry, where again it has been shown that S4R is the essential starting point for the formation of a variety of polyhedral clusters such as D4R and D6R.<sup>19</sup>

**Catalytic Studies.** In epoxidation reactions, titanium oxo clusters have been employed more often in comparison to the other types of titanium compounds, for the reason that titanium oxo clusters can be considered as model compounds for bulk  $\text{TiO}_2$ . Titanium oxo clusters are mostly carboxylate based and are synthesized from  $\text{Ti}(\text{OR})_4$  and  $\text{RCOOH}$ . In comparison, fewer titanium clusters have been reported starting from  $\text{Ti}(\text{OR})_4$  and  $\text{RPO}_3\text{H}_2/\text{R}_2\text{PO}_2\text{H}$ . These phosphorus-based titanium oxo clusters are generally pentacoordinated, whereas phosphorus-based stable hexacoordinated titanium oxo clusters are even fewer in the literature.<sup>4,21</sup> Titanium clusters with unreactive alkoxy groups are advantageous because they can give way for single-site heterogeneous catalysts in combination with silica. Single-site catalysts can establish a structure–activity relationship profile by eliminating the heterogeneity of active

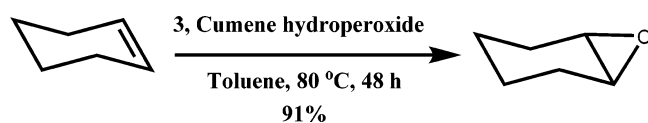
sites on the solid support. If the active sites are not uniform, multiple products can be expected in alkene epoxidation and therefore controlling active sites is very crucial for selective epoxidation. Among the epoxidation reactions, cyclohexene epoxidation has attracted more attention because of the industrial importance of its product, cyclohexene oxide.<sup>21</sup> Hence, it seems important to design new catalysts for selective cyclohexene epoxidation, which have single sites, are selective and are reusable along with having adequate catalytic activity.<sup>4,21</sup> Hexameric cluster **3** has been chosen in the present catalytic study due to the ease of isolating it as the pure product and its solubility in organic solvents. In contrast, the other clusters have poor solubility in organic solvents due to the presence of many  $-\text{OH}$  groups.

Using **3**, multiple trial reactions have been carried out employing diverse oxidants, solvents, temperatures, and catalytic amounts to achieve maximum conversion and selectivity. The obtained results are summarized in Table S6 in the Supporting Information. On the basis of our previous report,<sup>3a</sup> we have initially tried cyclohexene epoxidation with cumene hydroperoxide in toluene at 80 °C. It results in good cyclohexene conversion and selectivity in comparison to our previous results. To pick out the right catalyst dose, cyclohexene epoxidation has been carried out with three different catalyst doses (15, 30, and 60  $\mu\text{mol}$ ). As shown in Table S6, 30  $\mu\text{mol}$  is found to be the optimum catalytic dose to

reach maximum conversion with maximum selectivity. A catalytic amount either higher or lower than 30  $\mu\text{mol}$  decreases the cyclohexene conversion due to the deficient or crowded catalytic titanium centers. With an interest in green chemistry, less toxic oxidants (hydrogen peroxide and *tert*-butyl hydroperoxide) have also been utilized but resulted in only poor cyclohexene conversion.

Acetonitrile and toluene are the commonly reported solvents in the literature for cyclohexene epoxidation. Therefore, initially we have attempted cyclohexene epoxidation in toluene and acetonitrile. Toluene showed a better catalytic activity in comparison to acetonitrile. To find a suitable reaction temperature, four different temperatures (30, 60, 80, and 100  $^{\circ}\text{C}$ ) have been employed initially. Catalytic runs carried out at 30 and 60  $^{\circ}\text{C}$  resulted in only negligible and 63% cyclohexene conversion, respectively, even though maximum selectivity is obtained (99%). Maximum catalytic activity (91%) as well as epoxide selectivity (99%) has been accomplished at 80  $^{\circ}\text{C}$  after 48 h. However, cyclohexene epoxidation at 100  $^{\circ}\text{C}$  is found to be uncontrolled, as it shows reduced selectivity and decreased conversion (74%) (Scheme 8).

#### Scheme 8. Schematic Representation of Cyclohexene Epoxidation into Cyclohexene Epoxide



The catalytic activity of compound 3 has been also compared with that of the precursor ( $[\text{Ti}(\text{acac})_2(\text{O}^i\text{Pr})_2]$ ) under identical reaction conditions (Figure 6). The precursor compound

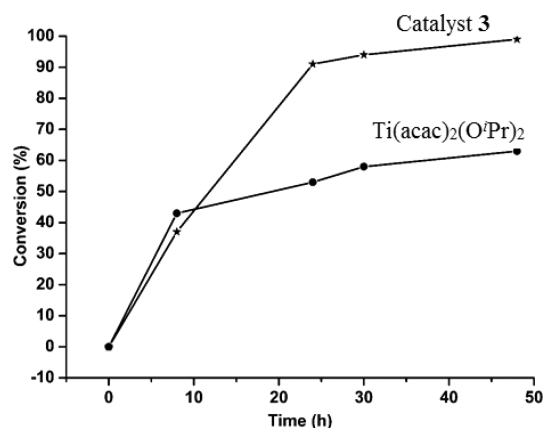


**Figure 6.** Comparison of catalytic activities of compound 3 and its precursor  $[\text{Ti}(\text{acac})_2(\text{O}^i\text{Pr})_2]$  under the optimized reaction conditions.

shows only 63% cyclohexene conversion after 48 h, but compound 3 shows 91% conversion. Two separate trial reactions have also performed, one without catalyst and one without oxidant. Both such trial reactions showed only negligible cyclohexene conversion, revealing that the obtained cyclohexene epoxidation is due to the combined function of catalyst and oxidant.

Complex 3 anchored on MCM-41 (50, 100, 150, or 200 mg of 3 with 500 mg of porous silica) results in four heterogeneous materials which have also been used as catalysts in cyclohexene

epoxidation using the optimized reaction conditions obtained from homogeneous catalysis.

Complex 3 anchored on MCM-41 (50, 100, 150, or 200 mg of 3 with 500 mg of porous silica) results in four heterogeneous catalysts ( $\text{TiP50@MCM-41}$ ,  $\text{TiP100@MCM-41}$ ,  $\text{TiP150@MCM-41}$ , and  $\text{TiP200@MCM-41}$ , respectively). The formation of these catalysts is supported by multiple characterization techniques (see the Supporting Information). Among these,  $\text{TiP200@MCM-41}$  has emerged as the best catalyst, exhibiting 67% conversion (93% selectivity to cyclohexene epoxide). Though the homogeneous catalyst 3 exhibits a better catalytic activity than  $\text{TiP@MCM-41}$  catalysts, the heterogeneous catalysts are still recommended due to their nondiminishing activity and reusability, even after five cycles (Figure 7).

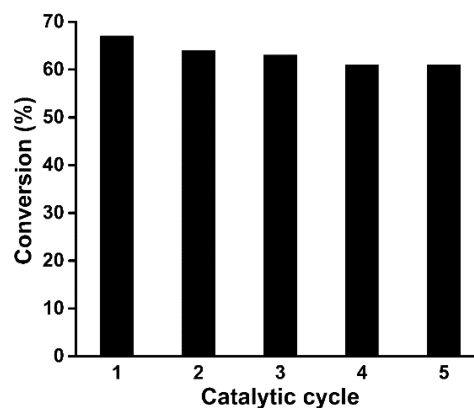


**Figure 7.** Reusability of  $\text{TiP200@MCM-41}$  over five consecutive catalytic runs under the optimized reaction conditions.

It is generally believed that the epoxidation reaction catalyzed by Ti-containing molecular sieves using peroxide oxidants occurs via four steps:<sup>22</sup> viz., (1) formation of Ti alkylperoxy species, (2) olefin activation, (3) the elimination of alcohol of the oxidant, and (4) formation of epoxide and regeneration of the catalyst. Since Ti catalysts  $\text{TiP@MCM-41}$  used in the present study are similar to other known titanosilicates, we believe that the catalysis here also follows the epoxidation mechanism as proposed above.

Under the optimized reaction conditions, epoxidation of a few more substrates (styrene, cyclooctene, 1-decene, and (-)  $\alpha$ -pinene) has also been performed using 3 and  $\text{TiP200@MCM-41}$ . Their activity and epoxide selectivity percent are given in Table S9 in the Supporting Information. The best conversion and selectivity have been accomplished in the epoxidation of cyclohexene in comparison to the other substrates.

## CONCLUSIONS

Extensive investigations pursued over a period of time in our laboratory on the reaction of  $[\text{Ti}(\text{acac})_2(\text{O}^i\text{Pr})_2]$  (I) with *tert*-butylphosphonic acid (II) have resulted in the isolation of as many as five different cluster entities which are structurally related to each other through a hierarchical growth mechanism. The reactions conducted between these two reactants in acetonitrile proved to be trickier than those conducted in dichloromethane medium. For example, preferential isolation of the products  $[\text{Ti}_4(\text{acac})_4(\mu\text{-O})_2(\mu\text{-}^i\text{BuPO}_3)_2(\mu\text{-}^i\text{BuPO}_3\text{H})_4] \cdot 2\text{C}_6\text{H}_5\text{CN}$  (1),  $[\text{Ti}_5(\text{acac})_5(\mu\text{-O})_2(\text{O}^i\text{Pr})_2(\mu\text{-}^i\text{BuPO}_3)_4(\mu\text{-}^i\text{BuPO}_3\text{H})_2]$  (2), and  $[\text{Ti}_6(\text{acac})_6(\mu\text{-O})_3(\text{O}^i\text{Pr})$

Table 1. Crystal Data and Structure Refinement Details for Complexes 1–5

	1	2	3	4	5
CCDC no.	1555092	1555091	1555093	1555094	1555090
formula	C <sub>48</sub> H <sub>92</sub> N <sub>2</sub> O <sub>28</sub> P <sub>6</sub> Ti <sub>4</sub>	C <sub>52</sub> H <sub>94</sub> O <sub>31</sub> P <sub>6</sub> Ti <sub>5</sub>	C <sub>60</sub> H <sub>110</sub> O <sub>34</sub> P <sub>6</sub> Ti <sub>6</sub>	C <sub>61</sub> H <sub>110</sub> N <sub>2</sub> O <sub>34</sub> P <sub>6</sub> Ti <sub>6</sub>	C <sub>58</sub> H <sub>104</sub> N <sub>2</sub> O <sub>34</sub> P <sub>6</sub> Ti <sub>6</sub>
fw	1522.65	1640.59	1848.69	1888.72	1846.65
temp, K	150(2)	150(2)	150(2)	150(2)	150(2)
cryst syst	monoclinic	monoclinic	monoclinic	monoclinic	triclinic
space group	P2 <sub>1</sub> /c	C2/c	P2 <sub>1</sub> /n	P2 <sub>1</sub> /c	P $\bar{1}$
a, Å	24.326(5)	25.4903(19)	15.781(6)	13.905(4)	13.853(2)
b, Å	19.900(3)	14.2195(8)	14.080(5)	16.815(5)	13.933(2)
c, Å	15.983(3)	25.1097(17)	20.897(7)	39.982(11)	14.393(3)
$\alpha$ , deg	90	90	90	90	103.6(1)
$\beta$ , deg	101.7(2)	115.7(3)	103.0(3)	95.8(2)	117.9(1)
$\gamma$ , deg	90	90	90	90	104.6(1)
V, Å <sup>3</sup>	7576.3(3)	8201.5(10)	4524(3)	9300(5)	2165.32(15)
Z	4	4	2	4	1
$\mu$ , mm <sup>-1</sup>	0.595	0.655	0.684	0.668	0.716
cryst size, mm <sup>3</sup>	0.20 × 0.20 × 0.20	0.24 × 0.20 × 0.20	0.10 × 0.07 × 0.04	0.19 × 0.17 × 0.03	0.20 × 0.17 × 0.12
$\theta$ range, deg	2.182–25.25	2.804–25.0	2.469–25.0	2.906–25.0	2.331–24.999
no. of rflns collected	58653	22551	30384	67890	23031
no. of indep rflns (I <sub>0</sub> > 2 $\sigma$ (I <sub>0</sub> ))	13705 (R(int) = 0.0559)	7188 (R(int) = 0.0582)	7954 (R(int) = 0.0370)	16329 (R(int) = 0.0615)	7499 (R(int) = 0.0697)
GOF	1.039	1.142	1.064	1.204	1.030
final R indices (I > 2 $\sigma$ (I))	R1 = 0.0778, wR2 = 0.1924	R1 = 0.1058, wR2 = 0.3039	R1 = 0.0513, wR2 = 0.1265	R1 = 0.0662, wR2 = 0.1314	R1 = 0.0557, wR2 = 0.1221
wR2 (all data)	0.2089	0.3354	0.1322	0.1361	0.1441
largest diff peak and hole, e Å <sup>-3</sup>	1.609 and -0.670	1.590 and -0.447	1.180 and -0.384	0.564 and -0.415	0.551 and -0.534

( $\mu$ -<sup>t</sup>BuPO<sub>3</sub>)<sub>5</sub>( $\mu$ -<sup>t</sup>BuPO<sub>3</sub>H)]·2CH<sub>3</sub>CN (4) from reactions between I and II in CH<sub>3</sub>CN requires strict 4:6, 5:6 and 1:1 stoichiometries of the reactants, respectively. This small difference in the initial stoichiometry has thus challenged us in isolating these products in pure form and characterizing them, which we have eventually managed to achieve. Particularly interesting is the isolation of the pentanuclear titanium phosphonate 2, which stands as the major testimony to the mechanism proposed. Although this cluster was expected to be asymmetric, the presence of a site occupancy related disorder around the fifth titanium center has further complicated the structural analysis, which was eventually resolved through a suitable model. Alternative strategies, such as switching over to less a hygroscopic solvent (CH<sub>2</sub>Cl<sub>2</sub>) to isolate [Ti<sub>6</sub>(acac)<sub>6</sub>(O<sup>i</sup>Pr)<sub>2</sub>( $\mu$ -O)<sub>2</sub>( $\mu$ -<sup>t</sup>BuPO<sub>3</sub>)<sub>6</sub>] (3) and changing the titanium source to [Ti(O)(acac)<sub>2</sub>] to characterize [Ti<sub>6</sub>(acac)<sub>6</sub>( $\mu$ -O)<sub>4</sub>( $\mu$ -<sup>t</sup>BuPO<sub>3</sub>)<sub>4</sub>( $\mu$ -<sup>t</sup>BuPO<sub>3</sub>H)<sub>2</sub>]·2CH<sub>3</sub>CN (5) (the final member of this hierarchical chain), have been successfully employed to fix the missing pieces of this jigsaw puzzle. The sequence of reactions in Scheme 7 gives an overall indication about the possible stepwise cluster growth in metal phosphonate chemistry. Current work in our laboratory is centered on testing this hierarchical cluster building approach employing organophosphate monoesters as ligands instead of phosphonic acids.

## EXPERIMENTAL SECTION

**Instruments and Methods.** All experiments were performed under an atmosphere of nitrogen using standard Schlenk line techniques. Solvents were dried using standard procedures and freshly distilled prior to use.<sup>23</sup> The melting points were measured in glass capillaries and are reported uncorrected. FT-IR spectra were obtained on a PerkinElmer Spectrum One FT-IR spectrometer as KBr diluted disks. Microanalyses were performed on a Thermo Finnigan (FLASH EA 1112) micro analyzer. Thermogravimetric analyses were carried

out with a PerkinElmer thermal analysis system, under a stream of nitrogen gas at a heating rate of 10 °C/min. <sup>t</sup>BuP(O)(OH)<sub>2</sub> has been synthesized by following a published procedure.<sup>24</sup> [Ti(acac)<sub>2</sub>(O<sup>i</sup>Pr)<sub>2</sub>] was obtained from Lancaster Chemicals U.K. and [Ti(O)(acac)<sub>2</sub>] from Sigma-Aldrich.

**Synthesis of Complex 1.** [Ti(acac)<sub>2</sub>(O<sup>i</sup>Pr)<sub>2</sub>] (0.8 mL, 2 mmol) was slowly added to a suspension of *tert*-butylphosphonic acid (0.414 g, 3 mmol) in acetonitrile (10 mL) at room temperature with stirring. The reaction mixture was stirred for 12 h at room temperature and filtered. Pale yellow crystals of [Ti<sub>4</sub>(acac)<sub>4</sub>( $\mu$ -O)<sub>2</sub>( $\mu$ -<sup>t</sup>BuPO<sub>3</sub>)<sub>2</sub>( $\mu$ -<sup>t</sup>BuPO<sub>3</sub>H)<sub>4</sub>]·2CH<sub>3</sub>CN (1) were formed over a period of 20 days at room temperature. Yield: 420 mg (55.2%, based on phosphonic acid); Mp: >250 °C. Anal. Calcd for C<sub>48</sub>H<sub>92</sub>N<sub>2</sub>O<sub>28</sub>P<sub>6</sub>Ti<sub>4</sub> (mol wt 1522.65): C, 37.87; H, 6.09; N, 1.84. Found: C, 38.99; H, 5.62; N, 1.48. FT-IR (KBr/cm<sup>-1</sup>): 1605 (s), 1527 (s), 1463 (vs), 1378 (vs), 1278 (w), 1139 (s), 1075 (s), 1022 (w), 992 (w), 722 (w), 657 (w). TGA: emperature range °C (% weight loss): 20–250 (s); 250–550 (48.2).

**Synthesis of Complex 2.** To a suspension of *tert*-butylphosphonic acid (0.414 g, 3 mmol) in acetonitrile (10 mL) was added [Ti(acac)<sub>2</sub>(O<sup>i</sup>Pr)<sub>2</sub>] (1.0 mL, 2.5 mmol) slowly at room temperature with stirring. The mixture was then stirred for 12 h and filtered to remove the insoluble particles. Pale yellow crystals of [Ti<sub>5</sub>(acac)<sub>5</sub>( $\mu$ -O)<sub>2</sub>(O<sup>i</sup>Pr)( $\mu$ -<sup>t</sup>BuPO<sub>3</sub>)<sub>4</sub>( $\mu$ -<sup>t</sup>BuPO<sub>3</sub>H)<sub>2</sub>] (2) were formed over a period of 7 days at room temperature. Yield: 440 mg (53.4%, based on phosphonic acid); Mp: >250 °C. Anal. Calcd for C<sub>52</sub>H<sub>94</sub>O<sub>31</sub>P<sub>6</sub>Ti<sub>5</sub> (mol wt 1640.59): C, 38.07; H, 5.78. Found: C, 36.46; H, 5.85. FT-IR (KBr/cm<sup>-1</sup>): 3447 (br), 2973 (s), 1611 (s), 1545 (w), 1360 (m), 1150 (s), 1091 (s), 663 (w).

**Synthesis of Complex 3.** To a suspension of *tert*-butylphosphonic acid (0.414 g, 3 mmol) in dichloromethane (10 mL) was slowly added [Ti(acac)<sub>2</sub>(O<sup>i</sup>Pr)<sub>2</sub>] (1.2 mL, 3 mmol) at room temperature with constant stirring. The reaction mixture was then stirred for 12 h and filtered to remove any insoluble particles. The clear solution was left for crystallization, from which pale yellow crystals of [Ti<sub>6</sub>(acac)<sub>6</sub>(O<sup>i</sup>Pr)<sub>2</sub>( $\mu$ -O)<sub>2</sub>( $\mu$ -<sup>t</sup>BuPO<sub>3</sub>)<sub>6</sub>] (3) formed over a period of 20 days at room temperature. Yield: 480 mg (52.6%, based on phosphonic acid). Mp: >250 °C. Anal. Calcd for C<sub>60</sub>H<sub>110</sub>O<sub>34</sub>P<sub>6</sub>Ti<sub>6</sub>

(mol wt 1848.69): C, 38.99; H, 6.00. Found: C, 39.23; H, 5.81. FT-IR (KBr/cm<sup>-1</sup>): 1596 (s), 1530 (s), 1466 (vs), 1377 (vs), 1280 (w), 1144 (s), 1050 (s), 1023 (w), 976 (w), 883 (w), 722 (s), 659 (s), 622 (w). TGA: temperature range °C (% weight loss): 20–250 (8); 250–550 (52.2).

**Synthesis of Complex 4.** To a suspension of *tert*-butylphosphonic acid (0.414 g, 3 mmol) in acetonitrile (10 mL) was slowly added [Ti(acac)<sub>2</sub>(O<sup>i</sup>Pr)<sub>2</sub>] (1.2 mL, 3 mmol) at room temperature with stirring. The reaction mixture was further stirred for 12 h and filtered to remove any insoluble particles. Pale yellow crystals of [Ti<sub>6</sub>(acac)<sub>6</sub>(μ-O)<sub>3</sub>(O<sup>i</sup>Pr)(μ<sup>-i</sup>BuPO<sub>3</sub>)<sub>5</sub>(μ<sup>-i</sup>BuPO<sub>3</sub>H)]<sub>2</sub>·2CH<sub>3</sub>CN (**4**) were formed from the clear filtrate over a period of 20 days at room temperature. Yield: 420 mg (45.0%, based on phosphonic acid). Mp: >250 °C. Anal. Calcd for C<sub>61</sub>H<sub>110</sub>N<sub>2</sub>O<sub>34</sub>P<sub>6</sub>Ti<sub>6</sub> (mol wt 1888.72): C, 38.79; H, 5.87; N, 1.48. Found: C, 39.33; H, 5.91; N, 1.88. FT-IR (KBr/cm<sup>-1</sup>): 1605 (s), 1527 (s), 1463 (vs), 1378 (vs), 1278 (w), 1139 (s), 1075 (s), 1022 (w), 992 (w), 722 (w), 657 (w). TGA: temperature range °C (% weight loss): 20–250 (8.1); 250–550 (31.9).

**Synthesis of Complex 5.** To a suspension of *tert*-butylphosphonic acid (138 mg, 1 mmol) in acetonitrile (15 mL) was added solid titanium oxy acetylacetonate ([Ti(acac)<sub>2</sub>(O)]); 262 mg, 1 mmol), and the mixture was stirred for 12 h. The resulting solution was filtered to obtain a clear yellow solution which resulted in yellow tiny crystals of the complex [Ti<sub>6</sub>(acac)<sub>6</sub>(μ-O)<sub>4</sub>(μ<sup>-i</sup>BuPO<sub>3</sub>)<sub>4</sub>(μ<sup>-i</sup>BuPO<sub>3</sub>H)]<sub>2</sub>·2CH<sub>3</sub>CN (**5**) at the bottom of the flask after 7 days. Yield: 110 mg (36.2%, based on phosphonic acid). Mp: >250 °C. Anal. Calcd for C<sub>58</sub>H<sub>104</sub>N<sub>2</sub>O<sub>34</sub>P<sub>6</sub>Ti<sub>6</sub> (mol wt 1846.65): C, 37.73; H, 5.68; N, 1.52. Found: C, 36.43; H, 5.22; N, 1.98. FT-IR (KBr/cm<sup>-1</sup>): 1597 (s), 1527 (s), 1480 (w), 1425 (w), 1381 (s), 1364 (s), 1279 (w), 1141 (s), 1041 (s), 1043 (s), 1024 (s), 992 (s), 945 (w), 834 (w), 798 (m), 707 (w), 658 (m), 538 (w), 499 (w), 433 (w). TGA: temperature range °C (% weight loss): 30–150 (5.5); 150–520 (43.1).

**Single-Crystal X-ray Diffraction Studies.** A suitable yellow crystal of **1** (size: 0.20 × 0.20 × 0.20 mm<sup>3</sup>) obtained directly from the reaction mixture was mounted on a Rigaku Saturn 724+ ccd diffractometer for the unit cell determination and three-dimensional intensity data collection. A total of 800 frames were collected at 150 K with an exposure time of 16 s per frame. For the analysis the detector distance was kept at 45 mm from the crystal. Data integration has been performed using CrysAlisPro software,<sup>25</sup> and all calculations were carried out using the programs in the WinGX module<sup>26</sup> and Olex 2.1<sup>27</sup> software by direct methods (SIR-97).<sup>28</sup> The final refinement of the structure was carried out using full least-squares methods on *F*<sup>2</sup> using SHELXL-2014.<sup>29</sup> Unit cell determinations using both high- and low-angle diffraction revealed that compound crystallizes in the monoclinic *P*2<sub>1</sub>/*c* space group. The final refinement converged at an *R* value of 0.0778 (*I* > 2σ(*I*)). Data collection and refinement of **2–5** were carried out similarly to that of **1**. The final refinement converged at an *R* value of 0.1058 (*I* > 2σ(*I*)) for **2**, 0.0513 (*I* > 2σ(*I*)) for **3**, 0.0662 (*I* > 2σ(*I*)) for **4**, and 0.0557 (*I* > 2σ(*I*)) for **5** (Table 1). Note: an earlier structure solution of compounds **3** and **4** has appeared in the CSD with REFCODEs MOSRAP and MOSRET, while more refined structures of these two compounds have now been submitted to CCDC as deposition numbers 1555093 and 1555094, respectively.<sup>30</sup>

## ■ ASSOCIATED CONTENT

### ● Supporting Information

The Supporting Information is available free of charge on the ACS Publications website at DOI: 10.1021/acs.inorgchem.7b01651.

Synthesis, crystallographic details, additional figures, and and spectral characterization (PDF)

### Accession Codes

CCDC 1555090–1555094 contain the supplementary crystallographic data for this paper. These data can be obtained free of charge via [www.ccdc.cam.ac.uk/data\\_request/cif](http://www.ccdc.cam.ac.uk/data_request/cif), or by email-

ing [data\\_request@ccdc.cam.ac.uk](mailto:data_request@ccdc.cam.ac.uk), or by contacting The Cambridge Crystallographic Data Centre, 12 Union Road, Cambridge CB2 1EZ, UK; fax: +44 1223 336033.

## ■ AUTHOR INFORMATION

### Corresponding Author

\*E-mail for R.M.: [rmv@chem.iitb.ac.in](mailto:rmv@chem.iitb.ac.in).

### ORCID

Sandeep Kumar Gupta: 0000-0003-2432-933X

Ramaswamy Murugavel: 0000-0002-1816-3225

### Funding

This work was supported by SERB, New Delhi (SB/S1/IC-48/2013 and SB/S2/JCB-85/2014).

### Notes

The authors declare no competing financial interest.

## ■ ACKNOWLEDGMENTS

R.M. thanks the SERB (SB/S2/JCB-85/2014) for a J. C. Bose Fellowship. K.S. and P.D. thank the CSIR for a research fellowship. S.K.G. thanks the SERB for research fellowship. R.A. thanks the DST SERB NPDF (PDF/2016/000037).

## ■ REFERENCES

- (1) (a) Murugavel, R.; Roesky, H. W. Titanosilicates: recent developments in synthesis and use as oxidation catalysts. *Angew. Chem., Int. Ed. Engl.* **1997**, *36*, 477–479. (b) Reddy, J. S.; Kumar, R.; Ratnasamy, P. Titanium silicalite-2: Synthesis, characterization and catalytic properties. *Appl. Catal.* **1990**, *58*, L1–L4. (c) Sheldon, R. A.; Van Doorn, J. A. Metal-catalyzed epoxidation of olefins with organic hydroperoxides: I. A comparison of various metal catalysts. *J. Catal.* **1973**, *31*, 427–437. (d) Kresge, C. T.; Leonowicz, M. E.; Roth, W. J.; Vartuli, J. C.; Beck, J. S. Ordered mesoporous molecular sieves synthesized by a liquid-crystal template mechanism. *Nature* **1992**, *359*, 710–712. (e) Cambor, M. A.; Costantini, M.; Corma, A.; Gilbert, L.; Esteve, P.; Martinez, A.; Valencia, S. Synthesis and catalytic activity of aluminium-free zeolite Ti-β oxidation catalysts. *Chem. Commun.* **1996**, 1339–1340. (f) Das, T. K.; Chandwadkar, A. J.; Sivasanker, S. A rapid method of synthesizing the titanium silicate ETS-10. *Chem. Commun.* **1996**, 1105–1106. (g) Liu, X.; Thomas, J. K. Synthesis of microporous titanosilicates ETS-10 and ETS-4 using solid TiO<sub>2</sub> as the source of titanium. *Chem. Commun.* **1996**, 1435–1436. (h) Tanev, P. T.; Chibwe, M.; Pinnavaia, T. J. Titanium-containing mesoporous molecular sieves for catalytic oxidation of aromatic compounds. *Nature* **1994**, *368*, 321–323. (i) Maschmeyer, T.; Rey, F.; Sankar, G.; Thomas, J. M. Heterogeneous catalysts obtained by grafting metallocene complexes onto mesoporous silica. *Nature* **1995**, *378*, 159–162.
- (2) (a) Chen, H. L.; Li, S. W.; Wang, Y. M. Synthesis and catalytic properties of multilayered MEL-type titanosilicate nanosheets. *J. Mater. Chem. A* **2015**, *3*, 5889–5900. (b) Ferdov, S. Layered titanosilicates for size- and pattern-controlled overgrowth of MFI zeolite. *CrystEngComm* **2014**, *16*, 4467–4471.
- (3) (a) Murugavel, R.; Davis, P.; Shete, V. S. Reactivity Studies, Structural Characterization, and Thermolysis of Cubic Titanosiloxanes: Precursors to Titanosilicate Materials Which Catalyze Olefin Epoxidation. *Inorg. Chem.* **2003**, *42*, 4696–4706. (b) Coles, M. P.; Lugmair, C. G.; Terry, K. W.; Tilley, T. D. Titania–Silica Materials from the Molecular Precursor Ti[OSi(OtBu)<sub>3</sub>]<sub>4</sub>: Selective Epoxidation Catalysts. *Chem. Mater.* **2000**, *12*, 122–131. (c) Fujiwara, M.; Wessel, H.; Park, H. S.; Roesky, H. W. A Sol–Gel Method Using Tetraethoxysilane and Acetic Anhydride: Immobilization of Cubic μ-Oxo Si–Ti Complex in a Silica Matrix. *Chem. Mater.* **2002**, *14*, 4975–4981. (d) Walawalkar, M. G.; Roesky, H. W.; Murugavel, R. Molecular Phosphonate Cages: Model Compounds and Starting Materials for Phosphate Materials. *Acc. Chem. Res.* **1999**, *32*, 117–126. (e) Vioux, A.; Le Bideau, J.; Mutin, P. H.; Leclercq, D., Hybrid organic-inorganic

- materials based on organophosphorus derivatives. In *New Aspects in Phosphorus Chemistry IV*; Springer: Berlin, 2004; pp 145–174.
- (f) Kumara Swamy, K. C.; Veith, M.; Huch, V.; Mathur, S. Structural Motifs in (t-butoxy) Zirconium Phosphinates, Arsenates, and Phosphates. *Inorg. Chem.* **2003**, *42*, 5837–5843.
- (4) Fang, W.-H.; Zhang, L.; Zhang, J. Synthetic investigation, structural analysis and photocatalytic study of a carboxylate-phosphonate bridged  $Ti_{18}$ -oxo cluster. *Dalton Trans.* **2017**, *46*, 803–807.
- (5) Walawalkar, M. G.; Horchler, S.; Dietrich, S.; Chakraborty, D.; Roesky, H. W.; Schäfer, M.; Schmidt, H.-G.; Sheldrick, G. M.; Murugavel, R. Novel organic-soluble molecular titanophosphonates with cage structures comparable to titanium-containing silicates. *Organometallics* **1998**, *17*, 2865–2868.
- (6) Pevec, A.; Demšar, A.; Pinkas, J.; Necas, M. Synthesis, spectroscopic and X-ray characterization of new molecular organotitanium(IV) phosphonate. *Inorg. Chem. Commun.* **2008**, *11*, 5–7.
- (7) Chakraborty, D.; Chandrasekhar, V.; Bhattacharjee, M.; Krätzner, R.; Roesky, H. W.; Noltemeyer, M.; Schmidt, H.-G. Metal Alkoxides as Versatile Precursors for Group 4 Phosphonates: Synthesis and X-ray Structure of a Novel Organosoluble Zirconium Phosphonate. *Inorg. Chem.* **2000**, *39*, 23–26.
- (8) (a) Mehring, M.; Guerrero, G.; Dahan, F.; Mutin, P. H.; Vioux, A. Syntheses, Characterizations, and Single-Crystal X-ray Structures of Soluble Titanium Alkoxide Phosphonates. *Inorg. Chem.* **2000**, *39*, 3325–3332. (b) Guerrero, G.; Mehring, M.; Mutin, P. H.; Dahan, F.; Vioux, A. Syntheses and single-crystal structures of novel soluble phosphonato- and phosphinato-bridged titanium oxo alkoxides. *J. Chem. Soc., Dalton Trans.* **1999**, 1537–1538.
- (9) Czakler, M.; Artner, C.; Schubert, U. Influence of the Phosphonate Ligand on the Structure of Phosphonate-Substituted Titanium Oxo Clusters. *Eur. J. Inorg. Chem.* **2013**, *2013*, 5790–5796.
- (10) Czakler, M.; Artner, C.; Schubert, U. Acetic Acid Mediated Synthesis of Phosphonate-Substituted Titanium Oxo Clusters. *Eur. J. Inorg. Chem.* **2014**, *2014*, 2038–2045.
- (11) Mutin, P. H.; Guerrero, G.; Vioux, A. Hybrid materials from organophosphorus coupling molecules. *J. Mater. Chem.* **2005**, *15*, 3761–3768.
- (12) Chen, Y.; Trzop, E.; Sokolow, J. D.; Coppens, P. Direct Observation of the Binding Mode of the Phosphonate Anchor to Nanosized Polyoxotitanate Clusters. *Chem. - Eur. J.* **2013**, *19*, 16651–16655.
- (13) Errington, R. J.; Ridland, J.; Willett, K. J.; Clegg, W.; Coxall, R. A.; Heath, S. L. Organophosphonate derivatives of titanium and niobium alkoxoanions. *J. Organomet. Chem.* **1998**, *550*, 473–476.
- (14) Thorn, D. L.; Harlow, R. L. Phosphato-titanium coordination chemistry. New phosphato-bridged chlorotitanium, imidotitanium, and oxotitanium compounds. *Inorg. Chem.* **1992**, *31*, 3917–3923.
- (15) Lugmair, C. G.; Tilley, T. D. Di-tert-butyl Phosphate Complexes of Titanium. *Inorg. Chem.* **1998**, *37*, 1821–1826.
- (16) (a) Kalita, L.; Kalita, A. C.; Murugavel, R. Organotitanium phosphates with free P–OH groups: Synthesis, spectroscopy and solid state structures. *J. Organomet. Chem.* **2014**, *751*, 555–562. (b) Murugavel, R.; Kuppaswamy, S. Organic-Soluble Tri-, Tetra-, and Pentanuclear Titanium(IV) Phosphates. *Inorg. Chem.* **2008**, *47*, 7686–7694.
- (17) Khou, C. B.; Dartt, C. B.; Labinger, J. A.; Davis, M. E. Studies on the Catalytic-Oxidation of Alkanes and Alkenes by Titanium Silicates. *J. Catal.* **1994**, *149*, 195–205.
- (18) (a) Brahmī, Y.; Katir, N.; Hameau, A.; Essoumhi, A.; Essassi, E. M.; Caminade, A.-M.; Bousmina, M.; Majoral, J.-P.; El Kadib, A. Hierarchically porous nanostructures through phosphonate-metal alkoxide condensation and growth using functionalized dendrimeric building blocks. *Chem. Commun.* **2011**, *47*, 8626–8628. (b) Jones, A. C.; Williams, P. A.; Bickley, J. F.; Steiner, A.; Davies, H. O.; Leedham, T. J.; Awaluddin, A.; Pemble, M. E.; Critchlow, G. W. Synthesis and crystal structures of two new titanium alkoxy-diolate complexes. Potential precursors for oxide ceramics. *J. Mater. Chem.* **2001**, *11*, 1428–1433.
- (19) (a) Gupta, S. K.; Kalita, A. C.; Dar, A. A.; Sen, S.; Patwari, G. N.; Murugavel, R. Elusive Double-Eight-Ring Zeolitic Secondary Building Unit. *J. Am. Chem. Soc.* **2017**, *139*, 59–62. (b) Dar, A. A.; Sharma, S. K.; Murugavel, R. Is single-4-ring the most basic but elusive secondary building unit that transforms to larger structures in zinc phosphate chemistry? *Inorg. Chem.* **2015**, *54*, 4882–4894. (c) Dar, A. A.; Sen, S.; Gupta, S. K.; Patwari, G. N.; Murugavel, R. Octanuclear Zinc Phosphates with Hitherto Unknown Cluster Architectures: Ancillary Ligand and Solvent Assisted Structural Transformations Thereof. *Inorg. Chem.* **2015**, *54*, 9458–9469. (d) Dar, A. A.; Bhat, G. A.; Murugavel, R. Dimensionality Alteration and Intra-versus Inter-SBU Void Encapsulation in Zinc Phosphate Frameworks. *Inorg. Chem.* **2016**, *55*, 5180–5190. (e) Murugavel, R.; Kuppaswamy, S.; Boomishankar, R.; Steiner, A. Hierarchical structures built from a molecular zinc phosphate core. *Angew. Chem., Int. Ed.* **2006**, *45*, 5536–5540. (f) Murugavel, R.; Kuppaswamy, S.; Gogoi, N.; Boomishankar, R.; Steiner, A. Noncovalent Synthesis of Hierarchical Zinc Phosphates from a Single  $Zn_4O_{12}P_4$  Double-Four-Ring Building Block: Dimensionality Control through the Choice of Auxiliary Ligands. *Chem. - Eur. J.* **2010**, *16*, 994–1009. (g) Murugavel, R.; Kuppaswamy, S.; Gogoi, N.; Steiner, A. Assembling Discrete D4R Zeolite SBUs through Noncovalent Interactions. 3.(1) Mediation by Butanols and 1, 2-Bis(dimethylamino) ethane. *Inorg. Chem.* **2010**, *49*, 2153–2162.
- (20) (a) Roesky, H. W.; Walawalkar, M. G.; Murugavel, R. Is Water a Friend or Foe in Organometallic Chemistry? The Case of Group 13 Organometallic Compounds. *Acc. Chem. Res.* **2001**, *34*, 201–211. (b) Walawalkar, M. G.; Murugavel, R.; Voigt, A.; Roesky, H. W.; Schmidt, H.-G. A Novel Molecular Gallium Phosphonate Cage Containing Sandwiched Lithium Ions: Synthesis, Structure, and Reactivity. *J. Am. Chem. Soc.* **1997**, *119*, 4656–4661. (c) Walawalkar, M. G.; Murugavel, R.; Roesky, H. W.; Usón, I.; Kraetzner, R. Gallophosphonates Containing Alkali Metal Ions. 2.1 Synthesis and Structure of Gallophosphonates Incorporating  $Na^+$  and  $K^+$  Ions. *Inorg. Chem.* **1998**, *37*, 473–478.
- (21) (a) Narayanam, N.; Chintakrinda, K.; Fang, W.-H.; Kang, Y.; Zhang, L.; Zhang, J. Azole Functionalized Polyoxo-Titanium Clusters with Sunlight-Driven Dye Degradation Applications: Synthesis, Structure, and Photocatalytic Studies. *Inorg. Chem.* **2016**, *55*, 10294–10301. (b) Liu, J.-X.; Gao, M.-Y.; Fang, W.-H.; Zhang, L.; Zhang, J. Bandgap Engineering of Titanium–Oxo Clusters: Labile Surface Sites Used for Ligand Substitution and Metal Incorporation. *Angew. Chem., Int. Ed.* **2016**, *55*, 5160–5165. (c) Jiang, Z.; Liu, J.; Gao, M.; Fan, X.; Zhang, L.; Zhang, J. Assembling Polyoxo-Titanium Clusters and CdS Nanoparticles to a Porous Matrix for Efficient and Tunable  $H_2$ -Evolution Activities with Visible Light. *Adv. Mater.* **2017**, *29*, 1603369.
- (22) (a) Ravasio, N.; Zaccheria, F.; Guidotti, M.; Psaro, R. Mono- and Bifunctional Heterogeneous Catalytic Transformation of Terpenes and Terpenoids. *Top. Catal.* **2004**, *27*, 157–168. (b) Zhang, X.; Wang, Y.; Xin, F. Coke deposition and characterization on titanium silicalite-1 catalyst in cyclohexanone ammoxidation. *Appl. Catal., A* **2006**, *307*, 222–230. (c) Mukherjee, S.; Samanta, S.; Bhaumik, A.; Ray, B. C. Mechanistic study of cyclohexene oxidation and its use in modification of industrial waste organics. *Appl. Catal., B* **2006**, *68*, 12–20. (d) Torres, J. C.; Cardoso, D.; Pereira, R. The influence of Si/Al and Si/Ti molar ratios of different [Ti, Al]-beta catalysts in the partial oxidation of cyclohexene with hydrogen peroxide. *Microporous Mesoporous Mater.* **2010**, *136*, 97–105. (e) Modak, A.; Nandi, M.; Bhaumik, A. Titanium containing periodic mesoporous organosilica as an efficient catalyst for the epoxidation of alkenes. *Catal. Today* **2012**, *198*, 45–51. (f) Bonino, F.; Damin, A.; Ricchiardi, G.; Ricci, M.; Spanò, G.; D'Aloisio, R.; Zecchina, A.; Lamberti, C.; Prestipino, C.; Bordiga, S. Ti-Peroxy Species in the TS-1/H<sub>2</sub>O<sub>2</sub>/H<sub>2</sub>O System. *J. Phys. Chem. B* **2004**, *108*, 3573–3583.
- (23) (a) Furniss, B. S. *Vogel's textbook of practical organic chemistry*; Pearson Education: Noida, India, 1989. (b) Armarego, W. L.; Chai, C.

L. L. *Purification of laboratory chemicals*; Butterworth-Heinemann: Oxford, U.K., 2013.

(24) Kinnear, A. M.; Perren, E. A. 661. Formation of organo-phosphorus compounds by the reaction of alkyl chlorides with phosphorus trichloride in the presence of aluminium chloride. *J. Chem. Soc.* **1952**, 3437–3445.

(25) *CrysAlisPRO*, O. D.; Agilent Technologies UK Ltd, Yarnton, England, 2012.

(26) Farrugia, L. WinGX suite for small-molecule single-crystal crystallography. *J. Appl. Crystallogr.* **1999**, *32*, 837–838.

(27) Dolomanov, O. V.; Bourhis, L. J.; Gildea, R. J.; Howard, J. A. K.; Puschmann, H. OLEX2: a complete structure solution, refinement and analysis program. *J. Appl. Crystallogr.* **2009**, *42*, 339–341.

(28) Altomare, A.; Burla, M. C.; Camalli, M.; Cascarano, G. L.; Giacovazzo, C.; Guagliardi, A.; Moliterni, A. G. G.; Polidori, G.; Spagna, R. SIR97: a new tool for crystal structure determination and refinement. *J. Appl. Crystallogr.* **1999**, *32*, 115–119.

(29) Sheldrick, G. M. Crystal structure refinement with SHELXL. *Acta Crystallogr., Sect. C: Struct. Chem.* **2015**, *71*, 3–8.

(30) Kalita, A. C.; Sharma, K.; Murugavel, (a) MOSRET, CCDC 1045314, *CSD Communication*, 2015; DOI:10.5517/cc142qtr. (b) MOSRAP, CCDC 1045313, *CSD Communication*, 2015; DOI:10.5517/cc142qsq.